

1 First evidence of Renlandian (c. 950-940 Ma) orogeny in  
2 Mainland Scotland: implications for the status of the Moine  
3 Supergroup and circum-North Atlantic correlations

4 Anna Bird<sup>1, 4</sup>, Kathryn Cutts<sup>2</sup>, Rob Strachan<sup>3</sup>, Matthew F. Thirlwall<sup>4</sup>, Martin Hand<sup>5</sup>

5 *<sup>1</sup> School of Environmental Sciences, University of Hull, Hull, HU6 7RX.*

6 <mailto:a.bird@hull.ac.uk>

7 *<sup>2</sup> Departamento de Geologia, Escola de Minas, Universidade Federal de Ouro Preto,  
8 Morro do Cruzeiro, 35400-000 Ouro Preto, MG, Brazil.*

9 *<sup>3</sup> School of Earth and Environmental Sciences, University of Portsmouth, Portsmouth*

10 *<sup>4</sup> Department of Earth Science, Royal Holloway; University of London, Egham, Surrey,  
11 TW20 0EX*

12 *<sup>5</sup> Department of Physical Sciences, University of Adelaide, Adelaide 5005, South  
13 Australia, Australia.*

14

15 **Abstract:**

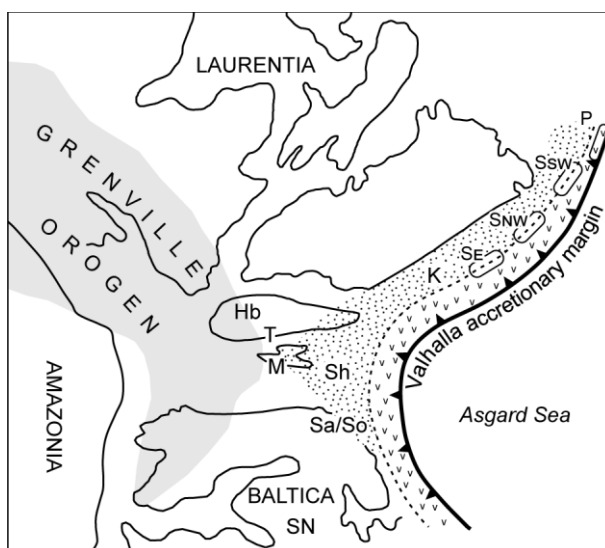
16 Central problems in the interpretation of the Neoproterozoic geology of the North  
17 Atlantic region arise from uncertainties in the ages of, and tectonic drivers for, Tonian  
18 orogenic events recorded in eastern Laurentia and northern Baltica. The identification  
19 and interpretation of these events is often problematic because most rock units that  
20 record Tonian orogenesis were strongly reworked at amphibolite facies during the  
21 Ordovician-Silurian Caledonian orogeny. Lu-Hf and Sm-Nd geochronology and  
22 metamorphic modelling carried out on large (>1cm) garnets from the Meadie Pelite in

23 the Moine Nappe of the northern Scottish Caledonides indicate prograde metamorphism  
24 between 950 - 940 Ma at pressures of 6-7 kbar and temperatures of 600°C. This  
25 represents the first evidence for c. 950 Ma Tonian (Renlandian) metamorphism in  
26 mainland Scotland and significantly extends its geographic extent along the palaeo-  
27 Laurentian margin. The Meadie Pelite is believed to be part of the Morar Group within  
28 the Moine Supergroup. If this is correct: 1) the Morar Group was deposited between 980  
29  $\pm$  4 Ma (age of the youngest detrital zircon; Peters, 2001, youngest published zircon  
30 date is  $947 \pm 189$  (Friend et al., 2003)) and c. 950 Ma (age of regional metamorphism  
31 reported here), 2) an orogenic unconformity must separate the Morar Group from the  
32  $883 \pm 35$  Ma (Cawood et al., 2004) Glenfinnan and Loch Eil groups, and 3) the term  
33 'Moine Supergroup' may no longer be appropriate. The Morar Group is broadly  
34 correlative with similar aged metasedimentary successions in Shetland, East  
35 Greenland, Svalbard, Ellesmere Island and northern Baltica. All these successions were  
36 deposited after c. 1030 Ma, contain detritus from the Grenville orogen, and were later  
37 deformed and metamorphosed at 950-910 Ma during accretionary Renlandian  
38 orogenesis along an active plate margin developed around this part of Rodinia.

### 39 **1. Introduction**

40 Interpretation of the Neoproterozoic geology of the North Atlantic region is problematic  
41 due to uncertainties in the ages of, and tectonic drivers for, Tonian metamorphic events  
42 recorded in parts of eastern Laurentia and northern Baltica. This causes ambiguity  
43 around the relative positioning of Laurentia and Baltica within the supercontinent  
44 Rodinia. In one palaeoreconstruction, Baltica is placed directly opposite East  
45 Greenland, and Tonian tectonometamorphic events in Svalbard, Norway, East

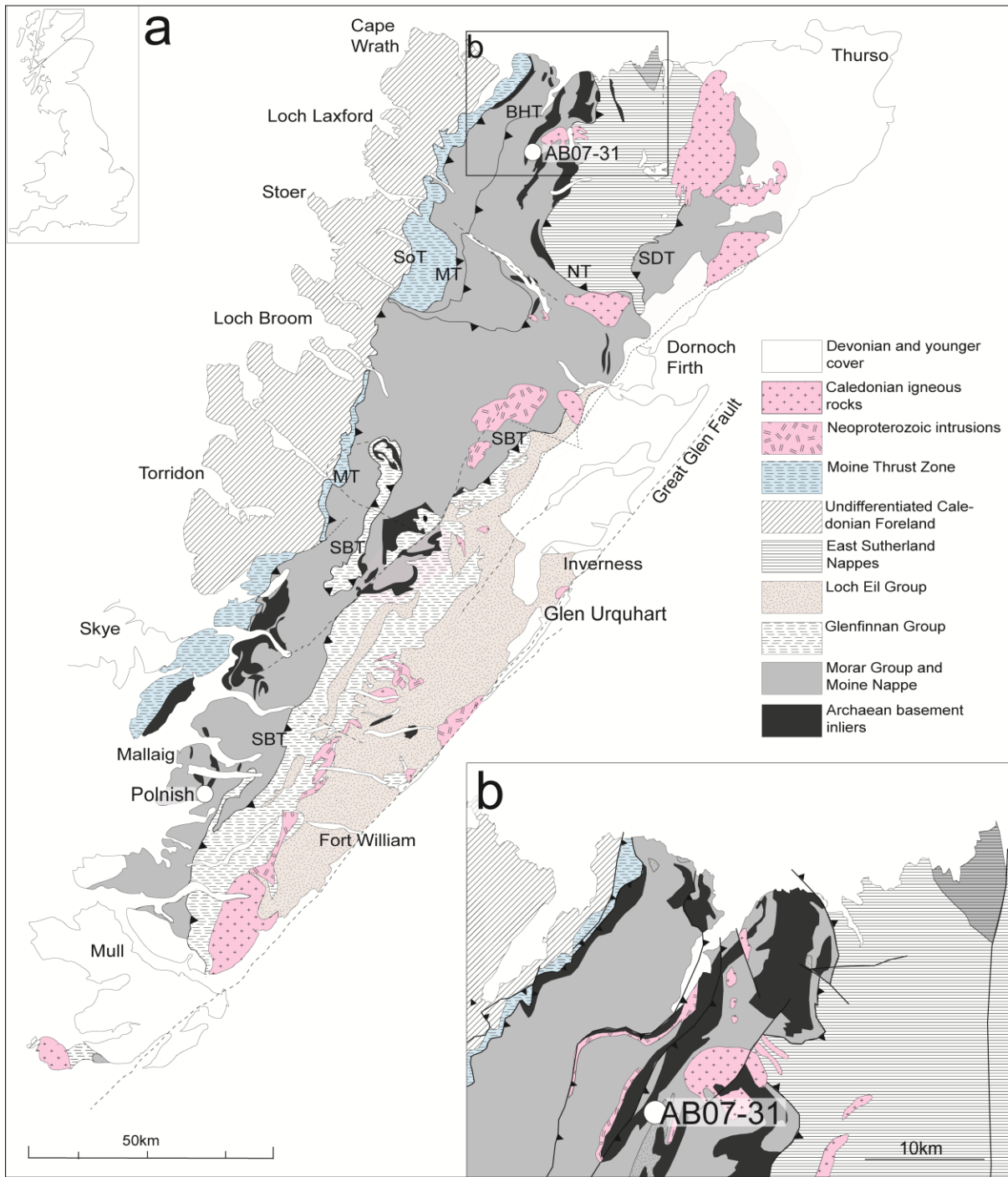
46 Greenland and Scotland at >900 Ma are regarded as collisional in nature, comprising a  
47 northern arm of the Grenville-Sveconorwegian orogen (Park 1992; Lorenz et al. 2012;  
48 Gee et al. 2015). In that context, younger tectonometamorphic events at 820-730 Ma in  
49 Scotland and Norway might represent the closure of intracratonic successor basins  
50 within Rodinia (Cawood et al. 2004). Alternatively, palaeomagnetic evidence (albeit  
51 fragmentary) supports the solution favoured here in which Baltica has a more southerly  
52 location relative to East Greenland (Fig 1; Elming et al., 2014; Li et al., 2008; Merdith et  
53 al. 2017; Pisarevsky et al., 2003; Cawood & Pisarevsky 2017). This places East  
54 Greenland, Svalbard, northern Norway and Scotland much closer to the periphery of  
55 Rodinia. An alternative hypothesis is therefore that Tonian deformation and  
56 metamorphism records the evolution of an external accretionary orogen developed  
57 above a continentward-dipping subduction zone (Fig 1; Cawood et al., 2010, 2015;  
58 Johansson, 2015; Kirkland et al., 2011; Malone et al., 2014, 2017). Cawood et al.  
59 (2010) termed this the 'Valhalla' orogen, distinguishing between >900 Ma 'Renlandian'  
60 and 820-725 Ma 'Knoydartian' orogenic events.



61

62 Fig. 1. Palaeogeographic reconstruction of the active peri-Laurentian-Baltican margin of Rodinia at c. 1100-1000 Ma (modified from Cawood et al.  
63 2010 and Malone et al. 2017). Shaded area represents the Grenville orogen. Dotted area represents marginal basins developed between the  
64 continental interior and a magmatic arc-subduction zone. Hb, Hebridean foreland; T, Torridon Group; M, Moine Supergroup; Sh, Shetland; Sa,  
65 Sværholt; So, Sørøy; K, Krummedal Succession; S<sub>E</sub>, East Svalbard; S<sub>NW</sub>, northwest Svalbard; S<sub>SW</sub>, southwest Svalbard; P, Pearya (Ellesmere Island).

66 Further advances in understanding the evolution of this orogenic tract depend in part  
67 upon acquisition of additional geochronological constraints coupled with pressure-  
68 temperature ( $P$ - $T$ ) data from metamorphic assemblages. However, the identification and  
69 interpretation of Tonian tectonometamorphic events within the North Atlantic  
70 borderlands is often problematic because many of the rock units that record orogenesis  
71 of this age were strongly reworked at amphibolite facies during the Ordovician-Silurian  
72 Caledonian orogeny. The degree of Caledonian over-printing means that information on  
73 the timing and pressure-temperature conditions of pre-Caledonian orogenic events is  
74 typically only preserved in the cores of garnet porphyroblasts (Vance et al. 1998; Cutts  
75 et al. 2009a; Cutts et al. 2009b; Cutts et al. 2010). In Shetland (Fig 1), a sillimanite  
76 foliation entirely preserved within garnet porphyroblasts gave U-Pb monazite and zircon  
77 ages of c. 950-940 Ma, despite the presence of kyanite-bearing Caledonian fabrics  
78 (Cutts et al. 2009b). In this paper we present the results of an integrated  
79 geochronological and metamorphic study of garnet porphyroblasts from the Meadie  
80 Pelite within the Caledonides of northern mainland Scotland (Fig 2). These results  
81 further extend the geographic range of Renlandian orogenic events, with implications for  
82 the ages of, and correlations between, major lithostratigraphic successions.



84

85  
86

Fig. 2 a. Simplified geological map of Scotland after Bird et al. 2013.. The location of AB07-31 is shown in Fig. 2a and in Fig 2b. Abbreviations; SBT – Sgurr Beag Thrust; MT – Moine Thrust; SoT – Sole Thrust; NT – Naver Thrust; BHT – Ben Hope Thrust; SDT, Skinsdale Thrust.

## 87 2. Regional Geology

88 The Caledonian orogenic belt in northern Scotland is limited to the west by the Moine  
89 Thrust (Fig 2). The Hebridean foreland comprises the Archaean-Palaeoproterozoic  
90 Lewisian Gneiss Complex which is overlain unconformably by three sedimentary  
91 successions: a) the c. 1200 Ma Stoer Group, b) the c. 1000 Ma Sleat and Torridon  
92 groups, and c) the Cambrian to Ordovician Ardvreck and Durness groups (e.g. Park et  
93 al. 2002 and references therein; Stewart 2002; Wheeler et al. 2010; Krabbendam et al.  
94 2008, 2017). In the hangingwall of the Moine Thrust, the metasedimentary rocks of the  
95 Moine Supergroup underlie large tracts of northern Scotland (Fig 2). Infolds and tectonic  
96 slices of Archaean orthogneisses have been broadly correlated with the Lewisian  
97 Gneiss Complex and are thought to represent the basement on which the Moine  
98 sediments were originally deposited (Ramsay 1958; Holdsworth 1989; Friend et al.  
99 2008).

100 The Moine Supergroup comprises the Morar, Glenfinnan and Loch Eil groups (Fig 2;  
101 Strachan et al. 2002, 2010 and references therein). All three groups record evidence for  
102 'Knoydartian' metamorphic events between 820 Ma and 725 Ma (Rogers et al. 1998;  
103 Vance et al. 1998; Tanner & Evans 2003 Cutts et al. 2009a, 2010; Cawood et al. 2015).  
104 The Morar Group was deposited after  $980 \pm 4$  Ma (the age of the youngest detrital  
105 zircon; Peters 2001) whereas the Glenfinnan and Loch Eil groups contain detrital  
106 zircons as young as  $885 \pm 85$  Ma (Cawood et al., 2004). Recent debate has centred on  
107 the stratigraphic relationship between the Morar Group and the Glenfinnan/Loch Eil  
108 groups. On Mull (Fig 2), the junction between the Morar and Glenfinnan groups has  
109 been interpreted as stratigraphic (Holdsworth et al. 1987). However, Krabbendam et al.

110 (2008) and Bonsor et al. (2012) favoured correlation of the Morar Group with the  
111 Torridon Group of the Hebridean foreland. The two successions were thought to have  
112 been deposited in the foreland basin to the c. 1.0 Ga Grenville orogen. If correct, this  
113 implies a depositional age close to c. 980 Ma for the Morar Group, which would  
114 therefore be distinctly older than the <885 Ma Glenfinnan and Loch Eil groups.  
115 Furthermore, the Morar Group would have been deposited prior to c. 940-925 Ma  
116 Renlandian metamorphism on Shetland (Cutts et al. 2009b; Cutts et al. 2011; Jahn et  
117 al. 2017), only 260 km north of mainland Scotland. If the Morar Group was affected by  
118 Renlandian orogenic activity, the Morar-Glenfinnan junction on Mull must hide a cryptic  
119 unconformity, and the term “Moine Supergroup” would be a misnomer. However, as yet  
120 no evidence has been forthcoming that would indicate that the Morar Group was  
121 affected by orogenesis of this age.

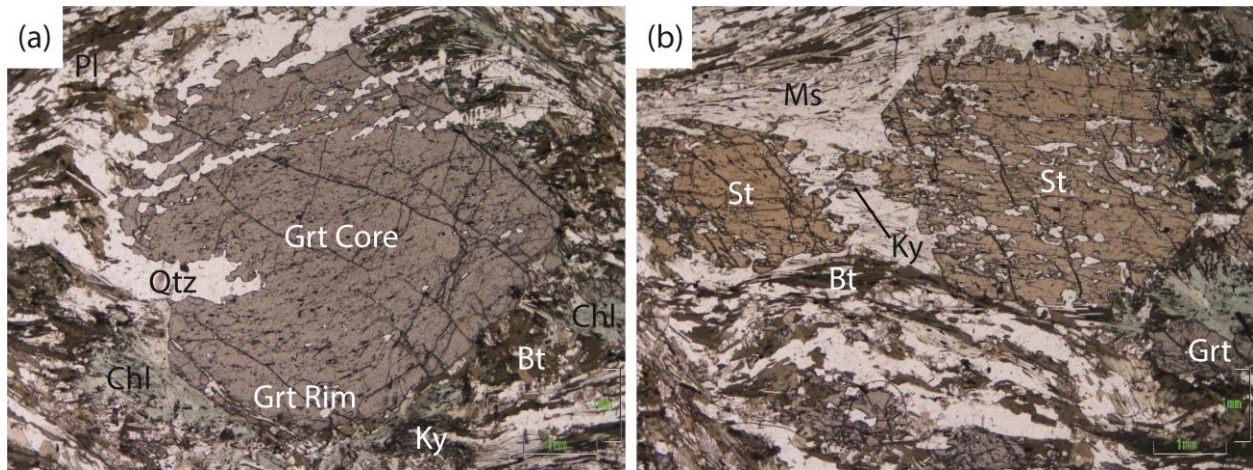
122 In Sutherland (northernmost mainland Scotland; Fig 2), the Morar Group is dominated  
123 by quartzo-feldspathic psammites with minor intercalations of pelitic schist (Moorhouse  
124 & Moorhouse 1988; Holdsworth 1989; Holdsworth et al. 2001). Inliers of Archaean  
125 basement mostly occur in the cores of large-scale anticlines. In central Sutherland (Fig  
126 2), the eastern part of the Meadie basement inlier is separated from typical Morar Group  
127 psammites by the Meadie Schist Formation. The latter comprises a lower semi-pelite  
128 (the ‘Meadie Schist’) and an upper garnetiferous pelite, locally with kyanite and  
129 staurolite (the ‘Meadie Pelite’). Although Moorhouse & Moorhouse (1988) assigned the  
130 Meadie Schist Formation to the pre-Moine basement, the unit does not contain any  
131 tectonic structures or metamorphic assemblages that are unequivocally older than the  
132 adjacent Moine rocks, and has no features in common with any undisputed basement

133 rocks in the area. Accordingly, the most recent interpretation of the area views the  
134 Meadie Schist Formation as a locally developed basal pelite of the Morar Group  
135 succession (British Geological Survey 2002).

### 136 **3. Sample Description**

137 Sample AB07-31 was obtained from the Meadie Pelite at NC 5231 4022 (Fig 2). The  
138 sample contains a well-developed muscovite-biotite foliation that is interpreted to be S2.  
139 The mica fabric is located within a quartz-plagioclase matrix and encloses garnet (1-20  
140 mm), staurolite (up to 30 mm) and kyanite (<1mm; Fig. 3a, b). Kyanite wraps garnet and  
141 staurolite as an S2 fabric element (Fig. 3a). Garnet grains contain inclusions of quartz  
142 and ilmenite, which preserve an earlier fabric (S1, in some grains this fabric appears to  
143 be crenulated) within garnet cores while garnet rims are often seen to have fewer  
144 inclusions than the cores (Fig. 3a). Staurolite grains have been observed to grow  
145 between the cores and rims of garnet; however it is uncertain whether these are  
146 inclusions or have grown at the expense of garnet. Fine grained garnet with extensive  
147 inclusions that are often oriented parallel to the matrix foliation grow around large garnet  
148 grains. Fine-grained kyanite, which is not oriented with the matrix foliation, is also found  
149 around the edges of large garnet grains (Fig. 3a). Large staurolite grains contain  
150 inclusions of ilmenite and quartz that are oriented in a crenulation fabric (Fig. 3b).  
151 Larger staurolite grains are often surrounded by kyanite with kyanite also growing along  
152 cracks within the staurolite grains (Fig. 3b). Finer grained, euhedral staurolite grains are  
153 present in the matrix where they truncate kyanite and muscovite grains. Randomly  
154 orientated chlorite occurs on the rims of the garnet and in the matrix biotite (Fig. 3b).





155

156

*Fig. 3. Photomicrographs of sample AB07-31. A. Large garnet showing inclusions and core and rim. B. Staurolite, with small garnets*

157

#### **4. Analytical Methods**

158

##### 4.1 Major and Trace Element Mineral Chemistry

159

Compositional traverses of garnet grains from sample AB07-31 were obtained using a

160

Cameca SX100 Electron Microprobe at the Open University. Quantitative analyses were

161

run at an accelerating voltage of 15 kV and a beam current of 20 nA, with a beam

162

diameter of 2-3  $\mu\text{m}$ . Analyses were collected on wavelength dispersive spectrometers

163

and all data is included in Supplementary File 1.

164

At Royal Holloway line traverses were carried out across the three garnets within a thick

165

(60 $\mu\text{m}$ ) thin-section of AB07-31. The instrumentation comprised a RESOLution L50

166

LPXPRO220 Excimer 193nm laser ablation system with a two-volume laser ablation cell

167

that was coupled to an Agilent 7500 ICP-MS (Müller et al., 2009).  $\text{SiO}_2$  contents

168

obtained by electron microprobe at the Natural History Museum were used as an

169

internal standard, and were found to be internally constant at  $37.7 \pm 0.21\%$ . Analysing

170

traverses of NIST SRM-612 glass standard at the beginning and end of each run

171

allowed for external standardization. The spot size for data acquisition was 44  $\mu\text{m}$ , the

172 repetition rate was 15 Hz, the scan speed was 0.5 mm/min. All LA ICP-MS data is  
173 included in Supplementary File 2.

174 The X-ray fluorescence (XRF) analyses were also undertaken at Royal Holloway using  
175 the methods described by Thirlwall et al. (2000).

## 176 4.2 Garnet Geochronology

177 Core and rim material was separated during picking based on a purple core and an  
178 orange rim. To calculate the amount of spike necessary to be added to the garnet  
179 fractions the Lu, Hf, Sm and Nd concentrations were estimated from part of the pure  
180 garnet using the LA ICP-MS trace element data (Fig 4). XRF analysis of whole rock  
181 powders was used to establish concentrations of Nd, Y and Zr to calculate the mass of  
182 spike needed for the whole rock fractions.

183 For Lu–Hf and Sm–Nd analyses, the procedures for sample leaching, spiking and  
184 dissolution generally followed the guidelines described by Anczkiewicz & Thirlwall  
185 (2003) and Bird et al. (2013). Lu-Hf and Sm-Nd analyses were performed on a single  
186 total dissolution. The samples were first passed through AG50W-X8 cation resin to  
187 separate high field strength elements (HFSE), light rare earth elements (LREE) and  
188 heavy rare earth elements (HREE) fractions. The HFSE fraction required a second pass  
189 through these columns to minimise the HREE that may be in the fraction. The fractions  
190 were individually passed through Eichrom LN resin to separate respectively Hf, Sm and  
191 Nd, and Lu. Total procedure blanks were typically 24pg for Hf and 23pg for Nd. The  
192 lowest Hf mass used is 62.2ng from sample from AB07-31 WR and when the effect  
193 from the blank is calculated for it has no significant effect on the age obtained from the

194 sample. This is also true for the sample with the lowest Nd mass is 64.1µg (AB07-31 Grt  
195 1).

196 Analyses conducted using the GV IsoProbe MC-ICP-MS at RHUL, follow procedures of  
197 Thirlwall & Anczkiewicz (2004), except that static mode was used. Blank solutions were  
198 analysed before each sample to provide on-peak-zeros, and yield < 0.07mV <sup>142</sup>Nd and  
199 0.08mV <sup>180</sup>Hf respectively, less than 10<sup>-3</sup> x typical sample intensities. Drift commonly  
200 observed in static ratio analysis required frequent analysis of JMC475 Hf and Aldrich Nd  
201 standards. Hf data were collected on two separate days, when JMC 475 yielded  
202 average <sup>176</sup>Hf/<sup>177</sup>Hf of 0.282189 ± 0.000009 and 0.282186 ± 0.000004 (2sd, N=6 and 5,  
203 respectively), and <sup>180</sup>Hf/<sup>177</sup>Hf of 1.88664 ± 0.00006 and 1.88679 ± 0.00005. Nd data  
204 were collected on three separate days, and on these Aldrich Nd and Aldrich mixed Nd  
205 Ce solutions yielded <sup>143</sup>Nd/<sup>144</sup>Nd of 0.511408 ± 0.000016, 0.511407 ± 0.000015 and  
206 0.511410 ± 0.000007, (2sd, N=11, 16 and 9 respectively), after slope correction using  
207 the method of Thirlwall & Anczkiewicz (2004). Isochron ages and uncertainties were  
208 calculated using Isoplot version 4.15 (Ludwig 2003) and decay constants of 1.865 x 10<sup>-11</sup>  
209 for <sup>176</sup>Lu (Scherer et al., 2001) and 6.54 x 10<sup>-12</sup> for <sup>147</sup>Sm (Gupta & Macfarlane 1970).

### 210 4.3 Metamorphic modelling

211 A pressure-temperature (*P-T*) pseudosection was calculated for sample AB07-31 using  
212 the composition obtained via whole-rock XRF analysis. *P-T* pseudosections were  
213 calculated using THERMOCALC v.3.33 (June 2009 update of Powell & Holland 1988)  
214 with the internally consistent dataset of Holland & Powell (1998; dataset tcds55,  
215 November 2003 update). *P-T* pseudosections were calculated for the geologically  
216 realistic system MnNCKFMASH (MnO–Na<sub>2</sub>O–CaO–K<sub>2</sub>O–FeO–MgO–Al<sub>2</sub>O<sub>3</sub>–SiO<sub>2</sub>–

217 H<sub>2</sub>O). The modelling for this system uses the *a*-*x* relationships of White et al. (2007) for  
218 silicate melt; Tinkham et al. (2001) for garnet, cordierite, staurolite and alkali feldspar;  
219 Powell and Holland (1999) for biotite and orthopyroxene; a combination of Mahar et al.  
220 (1997) and White et al. (2000) for chloritoid; Coggon & Holland (2002) for muscovite  
221 and paragonite; and Holland & Powell (2003) for plagioclase.

222 The constraint on maximum H<sub>2</sub>O content is taken as equivalent to the 'loss on ignition'  
223 from the XRF analyses. Compositional isopleths for garnet were calculated and have  
224 been plotted onto the peak field of the pseudosections to aid with interpretation of the  
225 *P*-*T* path.

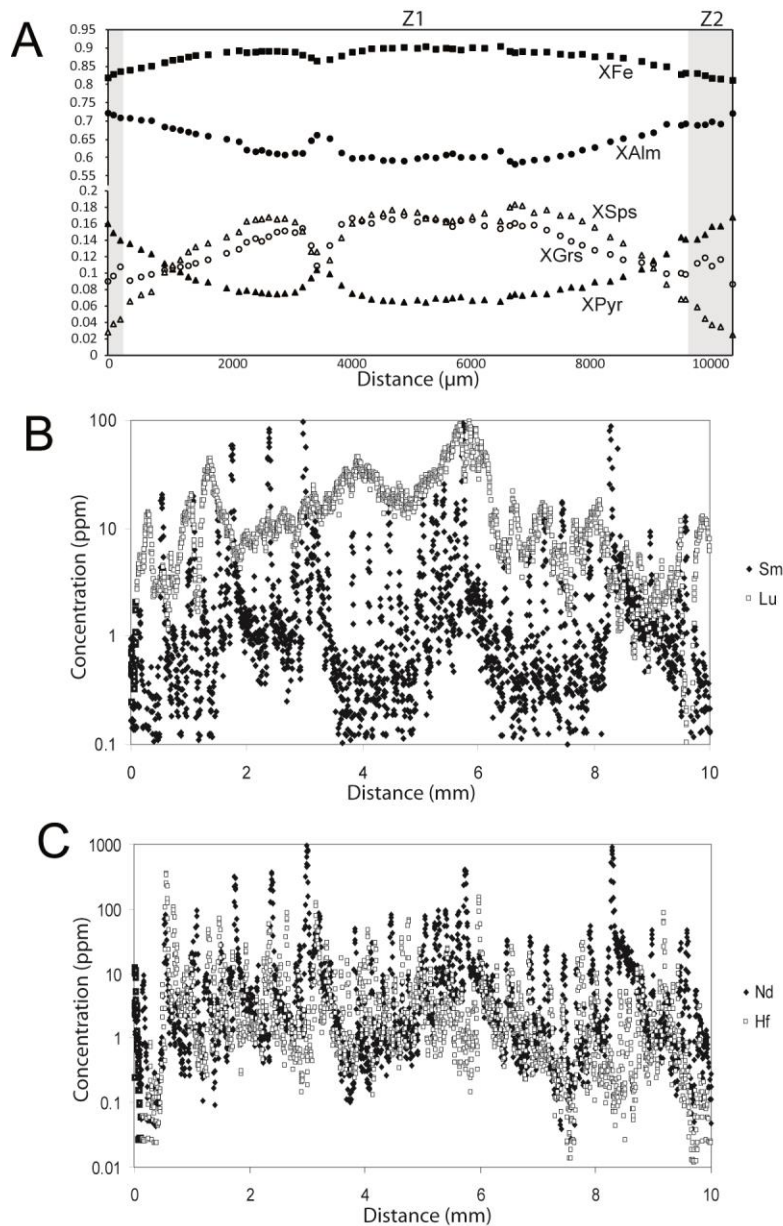
## 226 5. Results

### 227 5.1 Major and trace element garnet chemistry

228 Based on the electron microprobe traverses (Fig. 4A), garnet grains appear to have two  
229 compositional zones. Grain cores (Z1) are relatively rich in inclusions that are oriented  
230 in an S1 fabric (Fig. 3C). Compositionally, X<sub>Fe</sub>, X<sub>grs</sub> and X<sub>sps</sub> are highest in the core  
231 and drop toward the edge of Z1 (0.91-0.83, 0.17-0.09 and 0.18-0.06 respectively, Fig.  
232 4A). X<sub>pyr</sub> and X<sub>alm</sub> are lowest in the core and increase toward the edge of Z1 (0.06-  
233 0.14 and 0.59-0.70 respectively). On the edge of Z1 and Z2 there is a break in the  
234 compositional profiles of X<sub>Fe</sub>, X<sub>pyr</sub> and X<sub>sps</sub> and X<sub>grs</sub> (Fig. 4A). Zone Z2 contains  
235 fewer inclusions than the garnet cores (the exception being large staurolite grains which  
236 are occasionally included in this zone), where present, the inclusions again define an S1  
237 foliation. In Z2 X<sub>Fe</sub>, X<sub>grs</sub> and X<sub>sps</sub> drop towards the rim (0.83-0.81, 0.11-0.09 and 0.06-  
238 0.02 respectively) whereas X<sub>pyr</sub> and X<sub>alm</sub> rise towards the rim (0.14-0.17 and 0.70-  
239 0.73 respectively; Fig. 4A). There is no evidence of a change in composition on the very

240 rim of the garnet. However, in thin section the edges of garnet grains are abundant in  
241 inclusions and in some places are quite broken up and replaced by chlorite. In these  
242 areas, the orientation of inclusions is generally continuous with the matrix foliation.

243 Trace and major element data was also collected from AB07-31 garnet. The garnet  
244 shows notable HREE zoning, with HREE increasing towards the core, represented by  
245 Lu in Fig. 4B. Sm and Nd do not show any obvious zoning (Fig. 4B and C), but do show  
246 several peaks that relate to LREE and MREE-rich inclusions, e.g. apatite. Hf is fairly  
247 homogeneous throughout the garnet with some small peaks, which are probably due to  
248 minor zircon inclusions (Fig. 4C).



249

250 *Fig. 4. A. Major element traverse for sample AB07-31. B. Sm and Lu LA ICPMS profiles for AB07-31. C. Hf and Nd LA ICPMS profiles for AB07-31.*

251 **5.2 Garnet geochronology**

252 The dates reported in Table 1 are two-point dates based on a whole rock and garnet  
 253 fraction. Three Lu-Hf dates from the garnet core (Z1) are in the range 947.0 – 951.8 Ma  
 254 and consistent with one successful and slightly lower Lu-Hf rim date of  $942.1 \pm 4$  Ma  
 255 and also consistent with three low precision Sm-Nd dates ( $951$  to  $917 \pm 34$ - $32$  Ma). The

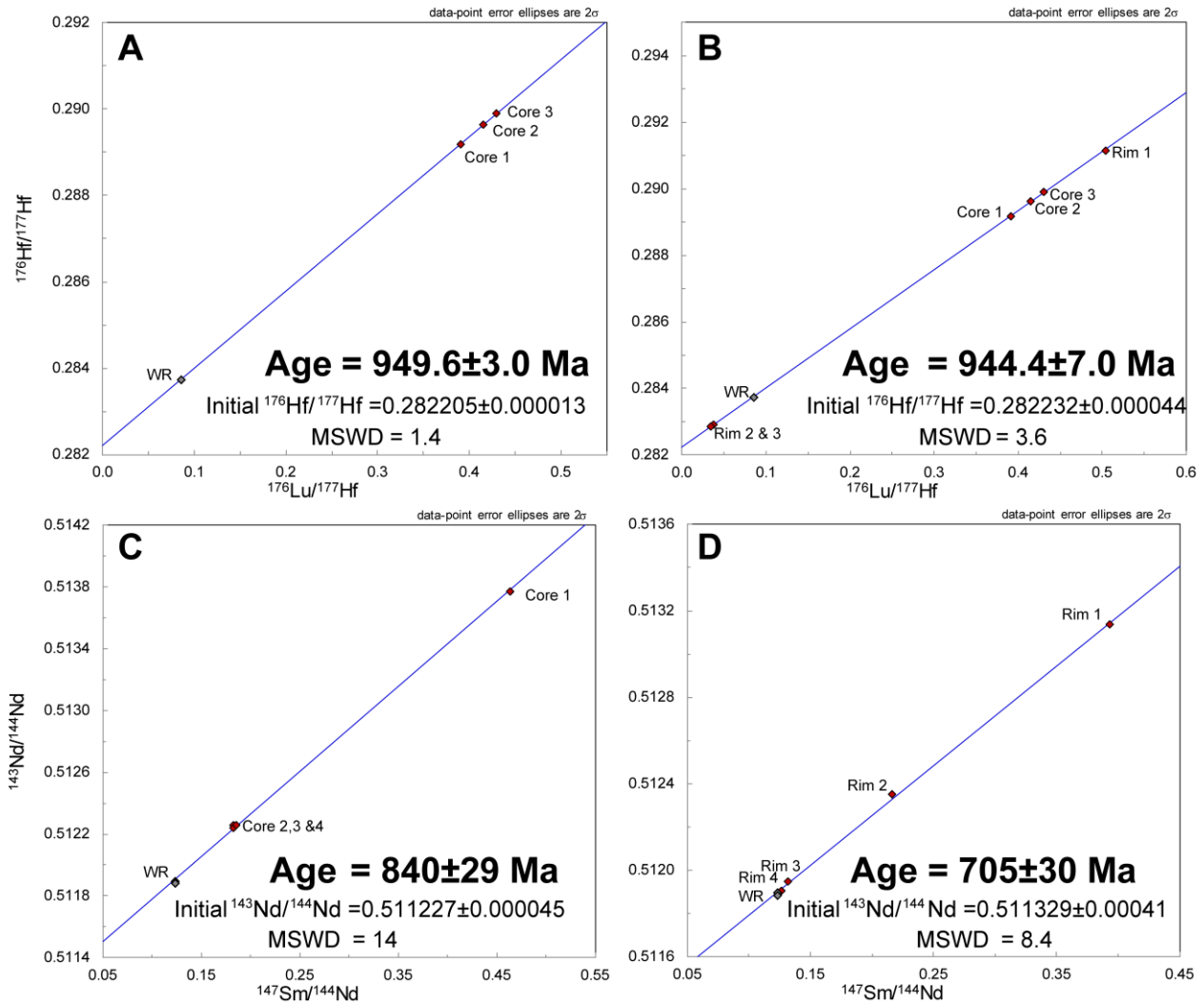
256 Lu-Hf core dates are considered robust as they have reasonably high  $^{176}\text{Lu}/^{177}\text{Hf}$  and  
 257  $^{176}\text{Hf}/^{177}\text{Hf}$  ratios and are within uncertainty of each other, they can also be calculated as  
 258 a 4-point isochron (Fig. 5A) using all three garnet cores and the whole-rock fraction to  
 259 give an date of  $949.6 \pm 3$  Ma (MSWD = 1.4). All the Lu-Hf data can be calculated as a 7-  
 260 point isochron of  $944.4 \pm 7.0$  (MSWD = 3.6), shown in Fig. 5B. Two further Lu-Hf rim  
 261 dates are within uncertainty of the core dates, but have poor precision, with  $^{176}\text{Lu}/^{177}\text{Hf}$   
 262 and  $^{176}\text{Hf}/^{177}\text{Hf}$  ratios lower than those of the whole rock, in part due to inclusions rich in  
 263 Hf, as the Hf concentrations are 75 and 6 ppm which the pure garnet is ~4 ppm (Table  
 264 1). Grt Core 1 gave a Sm-Nd date of  $841 \pm 9$  Ma. Gt Core samples 2, 3 and 4 have  
 265 large date errors due to low garnet  $^{147}\text{Sm}/^{144}\text{Nd}$  ratios, but are higher than the date for  
 266 Core 1, and within uncertainty of the Lu-Hf core dates suggesting that these ages may  
 267 be meaningful. The Sm-Nd dates from the garnet core can be calculated as a 5-point  
 268 isochron (Fig. 5C), which gives an age of  $840 \pm 29$  Ma (MSWD = 14). Two Sm-Nd rim  
 269 samples yield  $772 \pm 26$  Ma and  $701.7 \pm 9.7$  Ma, while another two yield dates that have  
 270 been strongly influenced by the presence of inclusions, shown by the high (6-53 ppm)  
 271 Nd concentrations, resulting in the garnets having similar  $^{147}\text{Sm}/^{144}\text{Nd}$  to the whole rock.

	LA ICPMS concentration (ppm)		Isotope ratios and concentrations determined by isotope dilution (ppm)									
	Lu	Hf	Lu	Lu 2se	Hf	Hf 2se	$^{176}\text{Lu}/^{177}\text{Hf}$	2se	$^{176}\text{Hf}/^{177}\text{Hf}$	2se	Age	2se
AB07-31 Grt Core 1	52.7	0.1	10.956	0.005	3.963	0.001	0.391	0.001	0.289179	0.000009	947.0	4.2
AB07-31 Grt Core 2	52.7	0.1	13.145	0.021	4.483	0.003	0.415	0.001	0.289631	0.000025	951.8	5.5
AB07-31 Grt Core 3	52.7	0.1	13.230	0.016	4.354	0.002	0.430	0.001	0.289897	0.000017	951.1	4.6
AB07-31 Grt Rim 1	17.0	0.3	14.031	0.033	3.942	0.004	0.504	0.002	0.291146	0.000010	942.1	3.7
AB07-31 Grt Rim 2	17.0	0.3	20.077	0.006	75.131	0.074	0.038	0.000	0.282914	0.000040	913	44
AB07-31 Grt Rim 3	17.0	0.3	1.556	0.001	6.457	0.007	0.034	0.000	0.282845	0.000038	917	39
AB07-31 WR	0.7	4.4	0.729	0.001	1.200	0.001	0.086	0.000	0.283738	0.000009		
	Sm	Nd	Sm	2se Sm	Nd	2se Nd	$^{147}\text{Sm}/^{144}\text{Nd}$	2se	143/144	2se	Age	2se
AB07-31 Grt Core 1	0.3	0.1	1.883	0.001	2.457	0.001	0.464	0.000	0.513771	0.000016	841.3	8.6
AB07-31 Grt Core 2	0.3	0.1	1.030	0.001	3.401	0.001	0.183	0.000	0.512256	0.000009	951	34

AB07-31 Grt Core 3	0.3	0.1	1.040	0.000	3.439	0.001	0.183	0.000	0.512241	0.000007	917	32
AB07-31 Grt Core 4	0.3	0.1	1.001	0.000	3.269	0.001	0.185	0.000	0.512260	0.000008	929	33
AB07-31 Grt Rim 1	0.8	0.2	1.696	0.000	2.608	0.001	0.393	0.000	0.513136	0.000013	701.7	9.7
AB07-31 Grt Rim 2	0.8	0.7	0.848	0.000	2.372	0.001	0.216	0.000	0.512353	0.000012	772	26
AB07-31 Grt Rim 3	0.8	0.7	11.674	0.005	53.539	0.027	0.132	0.000	0.511946	0.000012	1134*	28 0
AB07-31 Grt Rim 4	0.8	0.7	1.180	0.000	5.646	0.005	0.126	0.000	0.511905	0.000010	1098*	74 0
AB07-31 WR	6.2	30.9	5.330	0.002	26.083	0.002	0.124	0.000	0.511895	0.000012		
AB07-31 WR	6.2	30.9	5.462	0.002	26.755	0.002	0.123	0.000	0.511884	0.000010		

272  
273

Table 1, Lu-Hf and Sm-Nd geochronological data for sample AB07/31. The  $2\sigma$  uncertainty is less than 0.3% on  $^{176}\text{Lu}/^{177}\text{Hf}$ , and assumed to be 0.3% in the calculations. The  $2\sigma$  uncertainty is less than 0.1% on  $^{147}\text{Sm}/^{144}\text{Nd}$ , and assumed to be 0.1% in the calculations



274

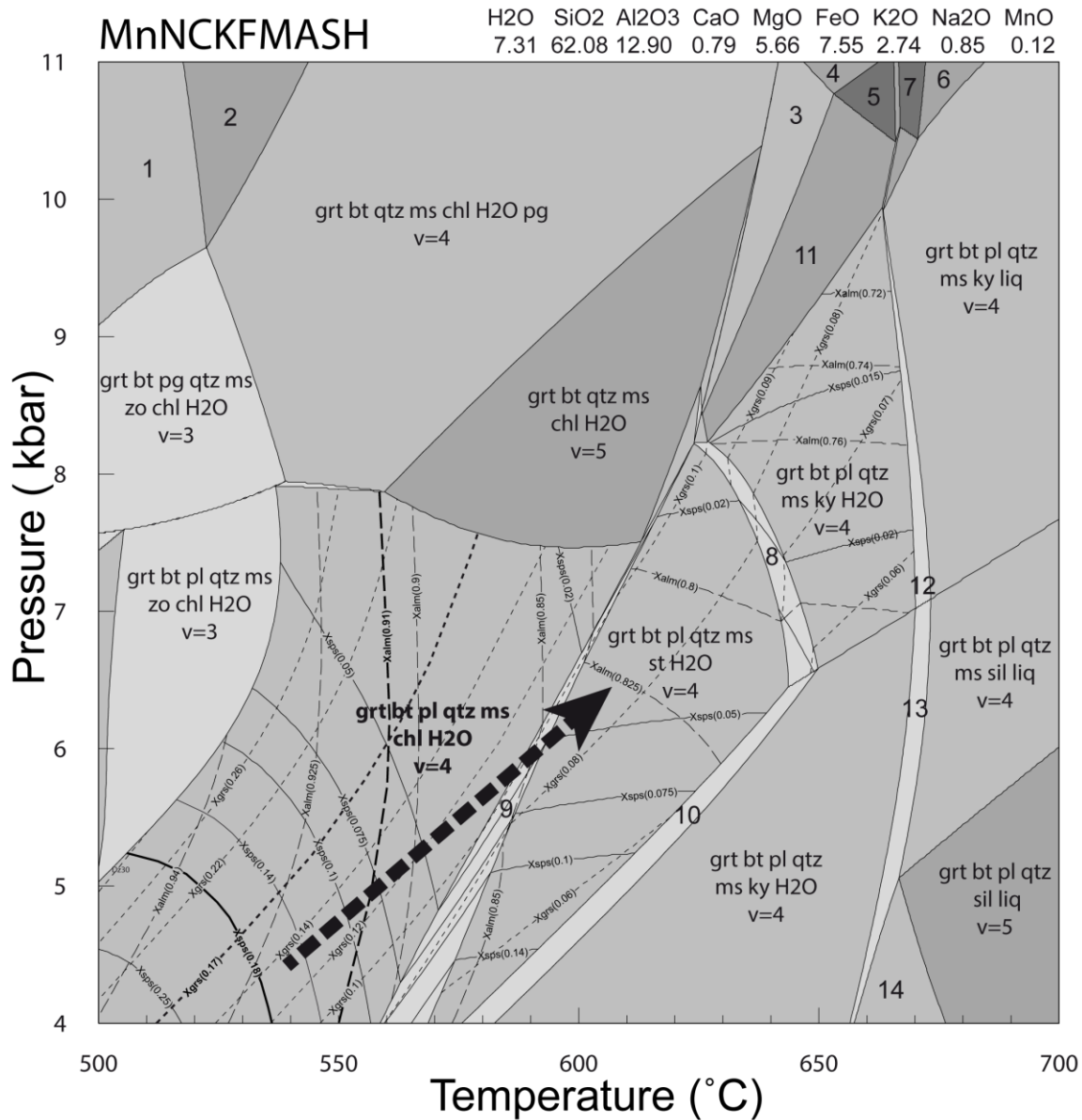
275  
276

Fig. 5. Lu-Hf and Sm-Nd isochrons for AB07-31. A shows the Lu-Hf isochron from the garnet core; B shows the Lu-Hf isochron using the core and rim fractions; C shows the Sm-Nd from the garnet core; and D shows the Sm-Nd isochron from the garnet rim.



### 277 5.3 Metamorphic modelling

278 The whole rock bulk composition was used to create the  $P$ - $T$  pseudosection, which  
279 shows the mineral relationships during the growth of Z1 garnet (Fig. 6). The  $P$ - $T$  path is  
280 defined by the mineral assemblage evolution as well as the chemical zoning profiles of  
281 each garnet zone. In the  $P$ - $T$  pseudosection, the garnet core composition overlaps in  
282 the field garnet + biotite + plagioclase + chlorite + muscovite + quartz which is  
283 consistent with the inclusion assemblage in the garnet grains. The change in  
284 composition of garnet in Z1 indicates an up- $P$  and  $T$  evolution into the staurolite-bearing  
285 field. This is consistent with the observation of multiple generations of staurolite in the  
286 sample. Peak conditions are difficult to determine, as it is possible that Z1 garnet rims  
287 were retrogressed prior to Z2 growth. A conservative estimate for this event is 6-7 kbar  
288 and c. 600 °C as there is no evidence of kyanite growth prior to growth of the Z2 garnet  
289 (Fig. 6).



- |  |   |
|--|---|
| 1. grt Qtz ms chl H <sub>2</sub> O pg zo | 8. grt bt pl Qtz ms st H <sub>2</sub> O ky    |
| 2. grt Qtz ms chl H <sub>2</sub> O pg    | 9. grt bt pl Qtz ms st H <sub>2</sub> O chl   |
| 3. grt bt Qtz ms H <sub>2</sub> O pg ky  | 10. grt bt pl Qtz ms st H <sub>2</sub> O sil  |
| 4. grt bt Qtz ms H <sub>2</sub> O pg     | 11. grt bt Qtz ms ky H <sub>2</sub> O         |
| 5. grt bt Qtz ms H <sub>2</sub> O        | 12. grt bt pl Qtz ms ky H <sub>2</sub> O liq  |
| 6. grt bt Qtz ms liq pl                  | 13. grt bt pl Qtz ms sil H <sub>2</sub> O liq |
| 7. grt bt Qtz ms liq                     | 14. grt bt pl Qtz sil liq H <sub>2</sub> O    |

290  
291  
292  
293

Fig. 6. The whole rock bulk composition was used to create a P-T pseudosection, for sample AB07-31. This diagram reflects mineral relationships during growth of Z1 garnet. The labelled, dashed lines indicate compositional isopleths for garnet. The bold ones indicate the composition of the garnet core. The large, dashed arrow indicates the P-T path for sample AB07-31 based on the compositional zoning in garnet.

## 294 6. Discussion and conclusions

### 295 6.1 Significance of age and P-T data

296 The LA ICP-MS gave a Hf concentration of ~1.7 ppm for pure garnet which is just  
297 less than half of the Hf concentration from isotope dilution in both of the garnet fractions.  
298 This suggests that there has been ~50% Hf contribution from zircon inclusions. The Nd  
299 concentration for pure garnet from LA ICP-MS was ~0.78 ppm, the Nd concentrations  
300 from ID ranged from 2.4 ppm to 3.4 ppm suggesting substantial input from Nd-rich  
301 inclusions. However, the two-point Sm-Nd dates from Gt core fractions 2, 3 and 4 are  
302 within uncertainty of the core Lu-Hf dates, suggesting that the inclusions have not  
303 significantly affected these dates, beyond reducing their precision. The ~100 Ma lower  
304 Sm-Nd date of Grt core 1 could represent physical mixing between the picked garnet  
305 core and rims as Sm-Nd rim dates are 200-180 Ma lower. Although, physical mixing  
306 should also affect the Lu-Hf dates, but it would have no observable effect as the Lu-Hf  
307 rim dates are nearly within error of the core dates. The lower Sm-Nd rim dates when  
308 compared with Lu-Hf may relate to differences in the closure temperatures between the  
309 two systems. Sm-Nd may have been partially reset by later Caledonian thermal events  
310 and not affect the Lu-Hf isotopic system, as Lu-Hf is thought to have a higher closure  
311 temperature than Sm-Nd (e.g. Anczkiewicz et al. 2007; Scherer et al., 2000; Smit et al.,  
312 2013).

313 The Electron Probe Micro Analysis (EPMA) data in combination with the Lu-Hf and Sm-  
314 Nd analyses suggests that the garnets have two growth zones (Fig. 4A). Based on the  
315 appearance of the garnet in thin section (broken up, thin rims with inclusions parallel to  
316 the matrix foliation as well as fine-grained matrix garnet), it is possible that there were

317 three episodes of garnet growth. Potentially, the cores and rims (zones 1 and 2) are  
318 Neoproterozoic while the thin rim and fine garnet could feasibly be Caledonian in age,  
319 which would correlate with the findings of Cutts et al. (2010) and Bird et al. (2013) from  
320 elsewhere within the Moine Supergroup. The LA-ICP-MS data can provide more  
321 information on whether the garnet dates reflect prograde growth or cooling, as samples  
322 with Lu enrichment towards the garnet cores (e.g. Fig. 4B) are more likely to provide  
323 dates that reflect garnet growth, as HREE are highly compatible in garnets (e.g. Lapen  
324 et al. 2003; Skora et al. 2008; Bird et al. 2013). Since this is the case here (Fig. 4B), the  
325 Lu-Hf dates presented here should reflect the age of garnet growth.

326 In summary, the data shows prograde garnet growth at ~950 Ma, relating to  
327 metamorphic pressures and temperatures of at least 6-7 kbar and 600°C. Z2 garnet  
328 probably grew during the same metamorphic event as it also overprints the S1 foliation  
329 and gives a similar age. The break in composition of the major elements could be a  
330 result of a growth hiatus, possibly as a result of the growth of staurolite (which appears  
331 as inclusions in Z2), limiting the amount of Al available for growth garnet (or even as a  
332 result of the growth of Z1 garnet altering the bulk composition of the sample, e.g. Cutts  
333 et al. (2010)). Z2 garnet also seems to have fewer quartz inclusions (Fig. 3a and  
334 Supplementary File 2), Kelly et al. (2015) found that quartz was consumed across the  
335 staurolite-in isograd, suggesting that Z2 garnet grew in equilibrium with staurolite. Z2  
336 achieved the highest-pressure conditions as matrix staurolite is partially replaced by  
337 kyanite (Figs. 3A, 6).

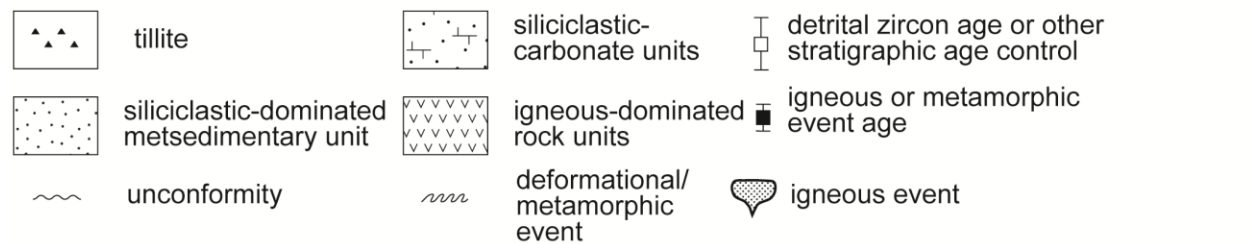
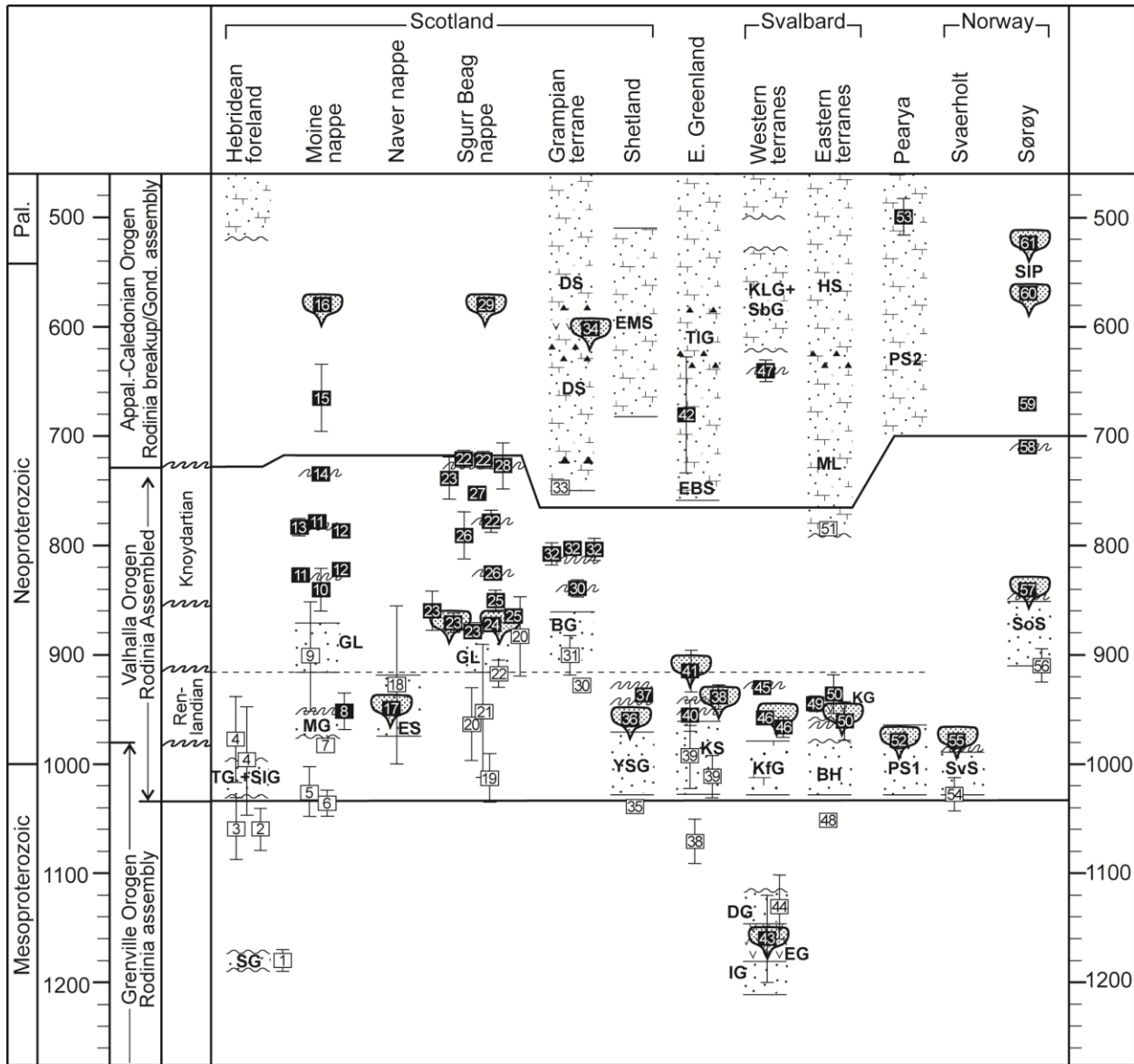
338 6.2. Implications for the status of the Moine Supergroup

339 Our findings potentially have significant implications for the age of the Morar  
340 Group and the status of the Moine Supergroup. If the Meadie Pelite is indeed part of the  
341 Morar Group as currently assumed, the latter must have been deposited between  $980 \pm$   
342  $4$  Ma (age of the youngest detrital zircon; Peters 2001) and c. 950-940 Ma (age of  
343 regional metamorphism reported here). Prior to the new ages reported here, the Morar  
344 Group was only constrained to have been deposited before  $842 \pm 20$  Ma, the age of  
345 new zircon rims on detrital grains (Kirkland et al. 2008). The data from the Meadie Pelite  
346 implies that an orogenic unconformity must separate the Morar Group from the  
347 Glenfinnan and Loch Eil groups that were deposited after  $883 \pm 35$  Ma (Cawood et al.,  
348 2004). As a 'supergroup' must comprise a number of groups that are linked by  
349 stratigraphic passage, the term 'Moine Supergroup' may therefore no longer be useful  
350 as it likely incorporates at least two unrelated sedimentary successions. Further isotopic  
351 and P-T data are necessary from Morar Group rocks higher in the succession in order  
352 to test this new view of Moine stratigraphy.

### 353 6.3 Correlations with other circum-North Atlantic successions

354 The data reported here provide the first evidence for c. 950-940 Ma Renlandian  
355 orogenic activity in mainland northern Scotland, significantly extending the geographic  
356 extent of this event southwards from Shetland. U-Pb zircon and monazite dates of c.  
357 950-930 Ma obtained from the Westing and Yell Sound groups and from reworked  
358 Archaean basement in northeast Shetland and interpreted to date prograde  
359 amphibolite-facies metamorphism (Cutts et al. 2009b; Jahn et al. 2017), are close to the  
360 new dates reported here. Further north along the palaeo-Laurentian margin of E  
361 Greenland, Svalbard and Ellesmere Island (Pearya, Fig 1) there is abundant evidence

362 for similar-aged tectonothermal activity (Figs 1 & 7; Cawood et al. 2010, 2015 and  
363 references therein). Evidence for amphibolite facies metamorphism and accompanying  
364 felsic magmatism at c. 950-910 Ma is recorded in the Krummedal Succession (E  
365 Greenland), the Krossfjorden Group (western Svalbard), the Brennevinsfjorden Group  
366 and Helvetesflya Formation (eastern Svalbard) and Pearya 'Succession I' (Pearya) (see  
367 references for Fig 7). The Sværholt Succession of northern Norway (Figs 1 & 7) is  
368 generally believed to be broadly time-equivalent, although deformation and  
369 metamorphism occurred slightly earlier at c. 980 Ma. All of these successions contain c.  
370 1100-1030 Ma populations of detrital zircons that are interpreted to have been sourced  
371 from the Grenville orogen (e.g. Cawood et al. 2007; Kirkland et al. 2008; Rainbird et al.  
372 2001, 2012). The temporal constraints provided by detrital zircon studies and dating of  
373 metamorphism and/or intrusive magmatism therefore imply that all these successions  
374 are broadly time-equivalent, although it is likely that they were deposited in separate  
375 basins. On the Scottish Hebridean foreland (Figs 1 & 7), the un-metamorphosed  
376 Torridon and Sleat groups are thought to form part of the same tectonostratigraphic  
377 package (Krabbendam et al. 2017 and references therein).



378  
379  
380  
381  
382  
383  
384  
385  
386  
387  
388  
389

**Figure 7.** Age range of principal late Mesoproterozoic to Palaeozoic metasedimentary units and of tectonothermal events within regions affected by the Valhalla Orogen, from the North Atlantic borderlands. See Supplementary File 3 for the extended figure caption. Numbers on data points refer to the following sources: 1 - Parnell et al. (2011); 2 - Rainbird et al. (2001); 3 - Krabbendam et al. (2017); 4 - Turnbull et al. (1996); 5 - Kirkland et al. (2008); 6 - Friend et al. (2003); 7 - Peters (2001); 8 - this paper; 9 - Cawood et al. (2015); 10 - Kirkland et al. (2008); 11 - Rogers et al. (1998); 12 - Vance et al. (1998); 13 - Cawood et al. (2015); 14 - Tanner and Evans (2003); 15 - Storey et al. (2004); 16 - Oliver et al. (2008); 17 - Kinny and Strachan (unpublished data); 18 - Friend et al. (2003); 19 - Kirkland et al. (2008); 20 - Cawood et al. (2004); 21 - Friend et al. (2003); 22 - Cutts et al. (2010); 23 - Cawood et al. (2015); 24 - (Friend et al., 1997), (Millar, 1999), (Rogers et al., 2001); 25 - Cawood et al. (2015); 26 - Cawood et al. (2015); 27 - Cawood et al. (2015); 28 - van Breemen et al. (1974); 29 - Kinny et al. (2003); 30 - Highton et al. (1999); 31 - Cawood et al. (2003); 32 - Noble et al. (1996); 33 - (Piasecki and van Breemen, 1983); 34 - Halliday et al. (1989) and Dempster et al. (2002); 35 - Cutts et al. (2009); 36 - Kinny and Strachan (unpublished data); 37 - Cutts et al. (2009 and Jahn et al. (2017); 38 - Watt et al. (2000); 39 - Kalsbeek et al. (2000); 40 - Strachan et al. (1995); 41 - Leslie and Nutman (2003); 42 - Jensen (1993); 43 - Balashov et al. (1996); 44 - Pettersson et al. (2009);

390 45 – Balashov et al. (1995); 46 – Pettersson et al. (2009); 47 – Majka et al. (2008); 48 – A.N. Larionov, unpub. data in Johansson et al. (2005); 49 –  
391 Johansson et al. (2000); 50 – Gee et al., (1995); see also Johansson et al., (2004); Johansson et al., (2000). 51 – Knoll (1982); 52 – Malone et al.  
392 (2017); 53 – Trettin et al. (1982); 54 – Kirkland et al. (2007); 55 – Kirkland et al. (2006); 56 – Kirkland et al. (2007); 57 – Kirkland et al. (2006); 58 –  
393 Kirkland et al. (2006); 59 – Kirkland et al. (2007); 60 – Roberts et al. (2006); 61 – Pedersen et al. (1989).

394 Abbreviations: BD – Badenoch Group; BH – Brennevsfjorden Group and Helvetesflya Formation; DG – Deilegga Group; DS – Dalradian  
395 Supergroup; EBS – Eleonore Bay Supergroup; EG – Eimfjellet Group; EMS – East Mainland Succession; ES – East Sutherland Moine succession; GL –  
396 Glenfinnan and Loch Eil groups; HS – Hinlopenstretet Supergroup; IG – Isbjørnhamma Group; KfG – Krossfjorden Group; KG – Kapp Hansteen  
397 Group; KLG – Kapp Lyell Group; KS – Krummedal succession; MG – Morar Group; ML – Murchisonfjorden and Lomfjorden successions; PS1 –  
398 Pearya Succession I; PS2 – Pearya Succession II; SbG – Sofiebogen Group; SG – Stoer Group; SIP – Seiland Igneous Province; SIG – Sleat Group; SoS  
399 – Sørøy succession, Kalak Nappe Complex; SvS – Svaerholt succession, Kalak Nappe Complex; TG – Torridon Group; TIG – Tillite Group; YSD – Yell  
400 Sound Division – Westing Group

401 In the context of the model of Cawood et al. (2010) for the Valhalla orogen (Fig  
402 1), potential tectonic drivers for Renlandian deformation and metamorphism are flat-slab  
403 subduction and /or terrane accretion. No allochthonous terranes have yet been  
404 identified but if present may be submerged on the rifted margins of the Arctic shelf. It is  
405 important to emphasise, however, that the conclusions of the present study do not  
406 preclude the interpretation that Renlandian events result from Laurentia-Baltica collision  
407 within a northern arm of the Grenville orogen as advocated by Park (1992), Lorenz et al.  
408 (2012) and Gee et al. (2015). Irrespective of which model is correct, post-920 Ma  
409 successor basins in Scotland (Glenfinnan, Loch Eil and Badenoch groups) and northern  
410 Baltica (Sørøy succession) likely resulted from steepening and/or retreat of subduction  
411 zones around this sector of Rodinia prior to renewed Knoydartian accretionary  
412 orogenesis at 820-725 Ma (Cawood et al. 2004, 2010, 2015).

#### 413 Acknowledgements

414 The authors would like to thank Dr Clare Warren for providing the electron microprobe  
415 data, Dr Christina Manning and Professor Wolfgang Müller data for access to the LA  
416 ICPMS. Acknowledgement also goes to NERC for funding Bird's PhD during which the  
417 majority of these analyses was undertaken, and to two anonymous reviewers who  
418 provided valuable insight.



419 References

- 420 Anczkiewicz, R. & Thirlwall, M. F. 2003. Improving precision of Sm-Nd garnet dating by  
421 H<sub>2</sub>SO<sub>4</sub> leaching: a simple solution to the phosphate inclusion problem. *In*: Vance, D.,  
422 Müller, W. & Villa, I. M. (eds) *Geochronology: Linking the Isotopic Record with Petrology*  
423 *and Textures*. Geological Society, London, Special Publications, 220, pp.83-91
- 424 Anczkiewicz R, Szczepanski J, Mazur S, Storey C, Crowley Q, Villa I, Thirlwall M,  
425 Jeffries T (2007) Lu-Hf geochronology and trace element distribution in garnet:  
426 implications for uplift and exhumation of ultra-high pressure granulites in the Sudetes,  
427 SW Poland. *Lithos* 95:363–380
- 428 Balashov, Y.A., Peucat, J.J., Teben'kov, A.M., Ohta, Y., Larionov, A.N., Sirotkin, A.N.,  
429 and Bjornerud, M., 1996, Rb-Sr whole rock and U-Pb zircon dating of the granitic-  
430 gabbroic rocks from the Skålfjellet Subgroup, southwest Spitsbergen: *Polar Research*,  
431 v. 15, p. 153-165.
- 432 Balashov, Y.A., Teben'kov, A.M., Ohta, Y., Larionov, A.N., Sirotkin, A.N., Gannibal, L.F.,  
433 and Ryunginen, G.I., 1995, Grenvillian U-Pb zircon ages of quartz porphyry and rhyolite  
434 clasts in a metaconglomerate at Vinsodden, southwestern Spitsbergen: *Polar Research*,  
435 v. 14, p. 291-302.
- 436 Bird, A.F., Thirlwall, M.F., Strachan, R.A., Manning, C.J., 2013. Lu – Hf and Sm – Nd  
437 dating of metamorphic garnet : evidence for multiple accretion events during the  
438 Caledonian orogeny in Scotland. , 170, pp.301–317
- 439 Bonsor, H.C. Strachan, R.A., Prave, A.R & Krabbendam, M. 2012. Sedimentology of the  
440 early Neoproterozoic Morar Group in northern Scotland: implications for basin models  
441 and tectonic setting. *Journal of the Geological Society*, 169(1), pp.53–65. Available at:  
442 <http://jgs.lyellcollection.org/cgi/doi/10.1144/0016-76492011-039>.
- 443 British Geological Survey. 2002. Loch Naver. Scotland Sheet 108E. Bedrock. 1:50,000  
444 Geology Series. Keyworth, Nottingham: British Geological Survey.
- 445 Cawood, P.A., Nemchin, A.A., Smith, M., and Loewy, S., 2003, Source of the Dalradian  
446 Supergroup constrained by U/Pb dating of detrital zircon and implications for the East  
447 Laurentian margin: *Journal of the Geological Society*, London, v. 160, p. 231-246.
- 448 Cawood, P.A., Nemchin, A.A., Strachan, R.A., Kinny, P.D. & Loewy, S. 2004.  
449 Laurentian provenance and an intracratonic tectonic setting for the Moine Supergroup,  
450 Scotland, constrained by detrital zircons from the Loch Eil and Glen Urquhart  
451 successions. *Journal of the Geological Society, London*, 161, pp.861-874.
- 452 Cawood, P.A., Strachan, R.A., Cutts, K.A., Kinny, P.D., Hand, M. & Pisarevsky, S.  
453 2010. Neoproterozoic orogeny along the margin of Rodinia: Valhalla orogen, North  
454 Atlantic. *Geology*, 38, pp.99-102. Cawood, P.A., Strachan, R.A., Merle, R.E., Millar, I.L.,

- 455 Loewy, S.L., Dalziel, I.W.D. & Connelly, J.N. 2015. Neoproterozoic to early Paleozoic  
456 extensional and compressional history of East Laurentian margin sequences: The  
457 Moine Supergroup, Scottish Caledonides. *Geological Society of America Bulletin*, 127,  
458 349–371.
- 459 Cawood, P.A. & Pisarevsky, S. 2017. Laurentia-Baltica-Amaozonia relations during Rodinia  
460 assembly. *Precambrian Research*, **292**, 386-397.
- 461 Coggon, R. & Holland, T. J. B., 2002. Mixing properties of phengitic micas and revised  
462 garnet-phengite thermobarometers. *Journal of Metamorphic Geology*, 20, 683–696.
- 463 Cutts, K.A., Hand, M., Kelsey, D.E. & Strachan, R.A. 2009a. Orogenic versus  
464 extensional settings for regional metamorphism: Knoydartian events in the Moine  
465 Supergroup revisited. *Journal of the Geological Society, London*, 166, pp. 201-204.
- 466 Cutts, K. A., Hand, M., Kelsey, D.E., Wade, B., Strachan., R.A., Clark., C. & Netting, A.  
467 2009b. Evidence for 930 Ma metamorphism in the Shetland Islands, Scottish  
468 Caledonides: implications for Neoproterozoic tectonics in the Laurentia-Baltica sector of  
469 Rodinia. *Journal of the Geological Society*, 166(6), pp.1033-1047.
- 470 Cutts, K.A., Kinny, P.D., Strachan, R.A., Hand, M., Kelsey, D.E., Emery, M., Friend,  
471 C.R.L. & Leslie, A.G. 2010. Three metamorphic events recorded in a single garnet:  
472 Integrated phase modelling, *in situ* LA-ICPMS and SIMS geochronology from the Moine  
473 Supergroup, Scotland. *Journal of Metamorphic Geology*, 28, pp.249-267.
- 474 Daly, J.S., Aitchison, S.J., Cliff, R.A., Gayer, R.A., and Rice, A.H.N., 1991,  
475 Geochronological evidence from discordant plutons for a Late Proterozoic orogen in the  
476 Caledonides of Finnmark, northern Norway: *Journal of the Geological Society, London*,  
477 v. 148, p. 29-40.
- 478 Dempster, T.J., Rogers, G., Tanner, P.W.G., Bluck, B.J., Muir, R.J., Redwood, S.D.,  
479 Ireland, T.R., and Paterson, B.A., 2002, Timing of deposition, orogenesis and glaciation  
480 within Dalradian rocks of Scotland: constraints from U-Pb zircon ages: *Journal of the*  
481 *Geological Society of London*, v. 159, p. 83-94.
- 482 Dhuime, B., Bosch, D., Bruguier, O., Caby, R., and Pourtales, S., 2007, Age,  
483 provenance and post-deposition metamorphic overprint of detrital zircons from the  
484 Nathorst Land group (NE Greenland)--A LA-ICP-MS and SIMS study: *Precambrian*  
485 *Research*, v. 155, p. 24-46.
- 486 Droop, G.T.R., 1987. A General Equation for Estimating Fe<sup>3+</sup> Concentrations in  
487 Ferromagnesian Silicates and Oxides from Microprobe Analyses, Using Stoichiometric  
488 Criteria. *Mineralogical Magazine*, 51(361), pp.431–435.

- 489 Elming, S.A., Pisarevsky, S.A., Layer, P., Bylund, G. 2014. A palaeomagnetic and  
490  $^{40}\text{Ar}/^{39}\text{Ar}$  study of mafic dykes in southern Sweden: A new Early Neoproterozoic key-  
491 pole for the Baltic Shield and implications for Sveconorwegian and Grenville loops.  
492 *Precambrian Research*, 244(1), pp.192–206. Available at:  
493 <http://dx.doi.org/10.1016/j.precamres.2013.12.007>.
- 494 Friend, C.R.L., Kinny, P.D., Rogers, G., Strachan, R.A., and Paterson, B.A., 1997, U-Pb  
495 zircon geochronological evidence for Neoproterozoic events in the Glenfinnan Group  
496 (Moine Supergroup): the formation of the Ardgour granite gneiss, north-west Scotland.:  
497 *Contributions to Mineralogy & Petrology*, v. 128, p. 101-113.
- 498 Friend, C.R.L., Strachan, R.A., Kinny, P., and Watt, G.R., 2003, Provenance of the  
499 Moine Supergroup of NW Scotland: evidence from geochronology of detrital and  
500 inherited zircons from (meta)sedimentary rocks granites and migmatites: *Journal of the*  
501 *Geological Society*, London, v. 160, p. 247-257.
- 502 Friend, C.R.L., Strachan, R. A. & Kinny, P.D., 2008. U-Pb zircon dating of basement  
503 inliers within the Moine Supergroup, Scottish Caledonides: implications of Archaean  
504 protolith ages. *Journal of the Geological Society*, 165(4), pp.807–815. Available at:  
505 <http://jgs.lyellcollection.org/cgi/doi/10.1144/0016-76492007-125> [Accessed August 14,  
506 2014].
- 507 Gee, D.G., Johansson, A., Ohta, Y., Tebenkov, A.M., Krasil'schikov, A.A., Balashov,  
508 Y.A., Larionov, A.N., Gannibal, L.F., and Ryungenen, G.I., 1995, Grenvillian basement  
509 and a major unconformity within the Caledonides of Nordaustlandet, Svalbard:  
510 *Precambrian Research*, v. 70, p. 215-234.
- 511 Gee, D.G. Andréassonb, P-G., Lorenza, H., Freic, D., Majka., J. 2015. Detrital zircon  
512 signatures of the Baltoscandian margin along the Arctic Circle Caledonides in Sweden:  
513 The Sveconorwegian connection. *Precambrian Research*, 265, pp.40–56. Available at:  
514 <http://dx.doi.org/10.1016/j.precamres.2015.05.012>.
- 515 Gupta, M. C., and R. D. MacFarlane. 1970. "The Natural Alpha Radioactivity of  
516 Samarium." *Journal of Inorganic and Nuclear Chemistry* 32 (11): 3425–32.
- 517 Halliday, A.N., Graham, C.M., Aftalion, M., and Dymoke, P., 1989, The deposition age  
518 of the Dalradian Supergroup: U-Pb and Sm-Nd isotopic studies of the Tayvallich  
519 Volcanics, Scotland: *Journal of the Geological Society*, London, v. 146, p. 3-6.
- 520 Highton, A.J., Hyslop, E.K., and Noble, S.R., 1999, U-Pb zircon geochronology of  
521 migmatization in the northern Central Highlands: evidence for pre-Caledonian  
522 (Neoproterozoic) tectonometamorphism in the Grampian block, Scotland: *Journal of the*  
523 *Geological Society*, London, v. 156, p. 1195-1204.
- 524 Holdsworth, R.E., Harris, A.L. & Roberts, A.M. 1987. The stratigraphy, structure and  
525 regional significance of the Moine rocks of Mull, Argyllshire, W Scotland. *Geological*  
526 *Journal*, 22, pp.83-107.

- 527 Holdsworth, R.E. 1989. The geology and structural evolution of a Caledonian fold and  
528 ductile thrust zone, Kyle of Tongue region, Sutherland, northern Scotland. *Journal of the*  
529 *Geological Society, London*, 146, pp.809-823.
- 530 Holdsworth, R.E., Strachan, R.A. & Alsop, G.I. 2001. Geology of the Tongue District.  
531 Memoir of the British Geological Survey, HMSO.
- 532 Holland, TJB, & Powell, R, 1998. An internally-consistent thermodynamic dataset for  
533 phases of petrological interest. *Journal of Metamorphic Geology* 16, 309–344.
- 534 Holland, T. J. B. & Powell, R., 2003. Activity–composition relations for phases in  
535 petrological calculations: an asymmetric multicomponent formulation. *Contributions to*  
536 *Mineralogy and Petrology*, 145, 492–501.
- 537 Jahn, I., Strachan, R.A., Fowler, M., Bruand, E., Kinny, P.D., Clark, C. & Taylor, R.J.M.  
538 2017. Evidence from U-Pb zircon geochronology for early Neoproterozoic (Tonian)  
539 reworking of an Archaean inlier in northeastern Shetland, Scottish Caledonides. *Journal*  
540 *of the Geological Society, London*, v. 174, p. 217-232.
- 541 Jensen, S.M., 1993, Lead isotope studies on mineral showings and ore deposits in East  
542 Greenland.: Grønlands geologiske Undersøgelse Rapport, v. 159, p. 101-108.
- 543 Johansson, A., Gee, D.G., Larionov, A.N., Ohta, Y., and Tebenkov, A.M., 2005,  
544 Grenvillian and Caledonian evolution of eastern Svalbard - a tale of two orogenies:  
545 *Terra Nova*, v. 17, p. 317-325.
- 546 Johansson, A., Larionov, A.N., Gee, D.G., Ohta, Y., Tebenkov, A.M., and Sandelin, S.,  
547 2004, Grenville and Caledonian tectono-magnetic activity in northeasternmost Svalbard,  
548 *in* Gee, D.G., and Pease, V.L., eds., *The Neoproterozoic Timanide Orogen of Eastern*  
549 *Baltica*: London, Geological Society, London, Memoirs, 30, p. 207-232.
- 550 Johansson, A., Larionov, A.N., Tebenkov, A.M., Gee, D.G., Whitehouse, M.J., and  
551 Vestin, J., 2000, Grenvillian magmatism of western and central Nordaustlandet,  
552 northeastern Svalbard: *Transactions of the Royal Society of Edinburgh, Earth Science*,  
553 v. 90, p. 221-254.
- 554 Johansson, Å., 2015. Comments to “Detrital zircon signatures of the Baltoscandian  
555 margin along the Arctic Circle Caledonides in Sweden: The Sveconorwegian  
556 connection” by Gee et al. (2015). *Precambrian Research*, 276, pp.233–235. Available  
557 at: <http://linkinghub.elsevier.com/retrieve/pii/S0301926815003800>.
- 558 Kalsbeek, F., Thrane, K., Nutman, A.P., and Jepsen, H.F., 2000, Late Mesoproterozoic  
559 to early Neoproterozoic history of the East Greenland Caledonides: evidence for  
560 Grenvillian orogenesis: *Journal of the Geological Society, London*, v. 157, p. 1215-1225.

- 561 Kalsbeek, F., Jepsen, H.F. & Nutman, A.P., 2001. From source migmatites to plutons:  
562 Tracking the origin of ca. 435 Ma S-type granites in the East Greenland Caledonian  
563 orogen. *Lithos*, 57(1), pp.1–21.
- 564 Kinny, P.D., Strachan, R.A., Kocks, H. and Friend, C.R.L., 2003, U-Pb geochronology of  
565 late Neoproterozoic augen granites in the Moine Supergroup, NW Scotland: dating of  
566 rift-related, felsic magmatism during supercontinent break-up?: *Journal of the*  
567 *Geological Society of London*, v. 160, p. 925-934.
- 568 Kirkland, C.L., Daly, J.S., and Whitehouse, M.J., 2006, Granitic magmatism of  
569 Grenvillian and late Neoproterozoic age in Finnmark, Arctic Norway--Constraining pre-  
570 Scandian deformation in the Kalak Nappe Complex: *Precambrian Research*, v. 145, p.  
571 24-52. —, 2007, Provenance and Terrane Evolution of the Kalak Nappe Complex,  
572 Norwegian Caledonides: Implications for Neoproterozoic Paleogeography and  
573 Tectonics: *Journal of Geology*, v. 115, p. 21-41.
- 574 Kirkland, C.L., Strachan, R.A., and Prave, A.R., 2008, Detrital zircon signature of the  
575 Moine Supergroup, Scotland: Contrasts and comparisons with other Neoproterozoic  
576 successions within the circum-North Atlantic region: *Precambrian Research*, v. 163, p.  
577 332-350.
- 578 Kirkland, C.L., Bingen, B., Whitehouse, M.J., Beyerd, E., Griffin, W.L. 2011.  
579 Neoproterozoic palaeogeography in the North Atlantic Region: Inferences from the  
580 Akkajaure and Seve Nappes of the Scandinavian Caledonides. *Precambrian Research*,  
581 186(1-4), pp.127–146. Available at: <http://dx.doi.org/10.1016/j.precamres.2011.01.010>.
- 582 Knoll, A.H., 1982, Microfossils from the Late Precambrian Dracén Conglomerate, Ny  
583 Friesland, Svalbard: *Journal of Paleontology*, v. 56, p. 755-790.
- 584 Krabbendam, M., Prave, T. & Cheer, D., 2008. A fluvial origin for the Neoproterozoic  
585 Morar Group, NW Scotland; implications for Torridon Morar Group correlation and the  
586 Grenville Orogen foreland basin. *Journal of the Geological Society*, 165(1), pp.379–394.  
587 Available at: <http://jgs.lyellcollection.org/cgi/doi/10.1144/0016-76492007-076> [Accessed  
588 August 14, 2014].
- 589 Krabbendam, M., Bonsor, H., Horstwood, M.S.A. & Rivers, T. 2017. Tracking the  
590 evolution of the Grenvillian foreland basin: Constraints from sedimentology and detrital  
591 zircon and rutile in the Sleat and Torridon groups, Scotland. *Precambrian Research*,  
592 295, 67-89.
- 593 Lapen, T. J., Johnson, C. M., Baumgartner, L. P., Mahlen, N. J., Beard, B. L. & Amato,  
594 J. M. 2003. Burial rates during prograde metamorphism of an ultra-high-pressure  
595 terrane: an example from Lago di Cignana, western Alps, Italy. *Earth and Planetary*  
596 *Science Letters*, 215, pp.57-72

- 597 Leslie, A.G. & Nutman, A.P., 2003, Evidence for Neoproterozoic orogenesis and early  
598 high temperature Scandian deformation events in the southern East Greenland  
599 Caledonides: *Geological Magazine*, 140, pp.309-333.
- 600 Lorenz, H., Gee, D.G., Larionov, A.N., Majka, J. 2012. The Grenville–Sveconorwegian  
601 orogen in the high Arctic. *Geological Magazine*, 149, pp 875-891.  
602 doi:10.1017/S0016756811001130
- 603 Li, Z.X., Bogdanova, S.V., Collins, A.S., Davidson, A., DeWaele, B., Ernst, R.E.,  
604 Fitzsimons, I.C.W., Fuck, R.A., Gladkochub, D.P., Jacobs, J., Karlstrom, K.E., Lu, S.,  
605 Natapov, L.M., Pease, V., Pisarevsky, S.A., Thrane, K., Vernikovskiy, V. 2008.  
606 Assembly, configuration, and break-up history of Rodinia: A synthesis. *Precambrian*  
607 *Research*, 160(1-2), pp.179–210.
- 608 Ludwig, K.R. 2010. Isoplot/Ex 3.00. National Science Foundation.
- 609 Mahar, E. M., Baker, J. M., Powell, R., Holland, T. J. B. & Howell, N., 1997. The effect  
610 of Mn on mineral stability in metapelites. *Journal of Metamorphic Geology*, 15, 223–238.
- 611 Majka, J., Mazur, S., Manecki, M., Czerny, J. and Holm, D.K. 2008. Late Neoproterozoic  
612 amphibolite-facies metamorphism of a pre-Caledonian basement block in southwest  
613 Wedel Jarlsberg Land, Spitzbergen: new evidence from U-Th-Pb dating of monazite.  
614 *Geological Magazine*, v. 145, p. 822-830.
- 615 Malone, S.J. McClelland, W.C., von Gosen, W., Piepjohn, K. 2014. Proterozoic  
616 Evolution of the North Atlantic–Arctic Caledonides: Insights from Detrital Zircon Analysis  
617 of Metasedimentary Rocks from the Pearya Terrane, Canadian High Arctic. *The Journal*  
618 *of Geology*, 122(6), pp.623–647. Available at:  
619 <http://www.jstor.org/stable/info/10.1086/677902>.
- 620 Malone, S.J., McClelland, W.C., von Gosen, W. & Piepjohn, K. 2017. The earliest  
621 Neoproterozoic magmatic record of the Pearya Terrane, Canadian High Arctic:  
622 implications for terrane reconstructions in the Arctic Caledonides. *Precambrian*  
623 *Research*, in press.
- 624 Merdith, A.S., Collins, A.S., Williams, S.E., Pisarevsky, S., Foden, J.D., Archibald, D.B.,  
625 Blades, M.L., Alessio, B.L., Armistead, S., Plavsa, D., Clark, C. & Müller, R.D. A full-  
626 plate global reconstruction of the Neoproterozoic. *Gondwana Research*, in press.
- 627 Millar, I.L., 1999, Neoproterozoic extensional basic magmatism associated with the  
628 West Highland granite gneiss in the Moine Supergroup of NW Scotland: *Journal of the*  
629 *Geological Society of London*, v. 156, p. 1153-1162.
- 630 Moorhouse, S.J. & Moorhouse, S.J. 1988. The Moine Assemblage in Sutherland. In:  
631 Winchester, J.A. (ed) *Later Proterozoic Stratigraphy of the Northern Atlantic Regions*.  
632 Blackie & Sons, Glasgow, pp.54-73.

- 633 Müller, W., Shelley, M., Miller, P., & Broude, S. 2009. Initial performance metrics of a  
634 new custom-designed ArF excimer LA-ICPMS system coupled to a two-volume laser-  
635 ablation cell. *Journal of Analytical Atomic Spectrometry*, **24**, pp.209-214.
- 636 Noble, S.R., Hyslop, E.K., and Highton, A.J., 1996, High-precision U-Pb monazite  
637 geochronology of the c. 806 Ma Grampian Shear Zone and the implications for the  
638 evolution of the Central Highlands of Scotland: *Journal of the Geological Society*,  
639 London, v. 153, p. 511-514.
- 640 Oliver, G.J.H., Wilde, S.A. and Wan, Y., 2008., Geochronology and dynamics of  
641 Scottish granitoids from the late Neoproterozoic break-up of Rodinia to Palaeozoic  
642 collision: *Journal of the Geological Society*, London, v. 165, p. 661-674.
- 643 Park, R.G. 1992. Plate kinematic history of Baltica during the Middle to Late  
644 Proterozoic: a model. *Geology*, **20**, 729-732.
- 645 Parnell, J., Mark, D., Fallick, A.E., Boyce, A. & Thackrey, S. 2011. The age of the  
646 Mesoproterozoic Stoer Group sedimentary and impact deposits, NW Scotland. *Journal*  
647 *of the Geological Society*, London, v. 168, p. 349-358.
- 648 Pedersen, R.B., Dunning, G.R., and Robins, B., 1989, U-Pb ages of nepheline syenite  
649 pegmatites from the Seiland Magmatic Province, north Norway, *in* Gayer, R.A., ed., *The*  
650 *Caledonide geology of Scandinavia*: London, Graham & Trotman, p. 3-8.
- 651 Peters, D. 2001. A geochemical and geochronological assessment of the Great Glen  
652 Fault as a terrane boundary. PhD thesis, University of Keele, UK.
- 653 Pettersson, C.H., Tebenkov, A.M., Larionov, A.N., Andresen, A.A., and Pease, V., 2009,  
654 Timing of migmatization and granite genesis in the Northwestern Terrane of Svalbard,  
655 Norway: implications for regional correlations in the Arctic Caledonides: *Journal of the*  
656 *Geological Society*, v. 166, p. 147-158.
- 657 Piasecki, M.A.J., and van Breemen, O., 1983, Field and isotope evidence for a c.750  
658 Ma tectonothermal event in Moine rocks in the Central Highland region of the Scottish  
659 Caledonides: *Transactions of the Royal Society of Edinburgh*, v. 73, p. 119-134.
- 660 Pisarevsky, S. A. WINGATE, M.T.D., POWELL, C., JOHNSON, S. EVANS, D.A.D 2003.  
661 Models of Rodinia assembly and fragmentation. *Geological Society, London, Special*  
662 *Publications*, 206(1), pp.35–55.
- 663 Powell, R., & Holland, TJB, 1988 An internally consistent thermodynamic dataset with  
664 uncertainties and correlations: 3: application methods, worked examples and a  
665 computer program. *Journal of Metamorphic Geology* 6, 173–204.

- 666 Powell, R, & Holland, TJB, 1999. Relating formulations of the thermodynamics of min-  
 667 eral solid solutions: activity modelling of pyroxenes, amphiboles and micas. *American*  
 668 *Mineralogist* 84, 1–14.
- 669 Rainbird, R.H., Hamilton, M.A., and Young, G.M., 2001, Detrital zircon geochronology  
 670 and provenance of the Torridonian, NW Scotland: *Journal of the Geological Society of*  
 671 *London*, v. 158, p. 15-27.
- 672 Rainbird, R.H., Cawood, P.A. & Gehrels, G. 2012. The great Grenvillian sedimentation  
 673 episode: record of supercontinent Rodinia's assembly. In: Busby, C. & Azor, A. (eds)  
 674 *Tectonics of Sedimentary Basins: Recent Advances*. Blackwell Publishing, 583-601.
- 675 Ramsay, J.G. 1958. Moine-Lewisian relations at Glenelg, Inverness-shire. *Quarterly*  
 676 *Journal of the Geological Society of London*, **113**, 487-523.
- 677 Roberts, R.J., Corfu, F., Torsvik, T.H., Ashwal, L.D., and Ramsay, D.M., 2006, Short-  
 678 lived mafic magmatism at 570 Ma in the northern Norwegian Caledonides: U/Pb zircon  
 679 ages
- 680 Rogers, G., Hyslop, E.K., Strachan, R.A., Paterson, B.A. & Holdsworth, R.E. 1998. The  
 681 structural setting and U-Pb geochronology of Knoydartian pegmatites in W. Inverness-  
 682 shire: evidence for Neoproterozoic tectonothermal events in the Moine of NW Scotland.  
 683 *Journal of the Geological Society, London*, **155**, 685-696.
- 684 Rogers, G., Kinny, P.D., Strachan, R.A., Friend, C.R.L., and Paterson, B.A., 2001, U-Pb  
 685 geochronology of the Fort Augustus granite gneiss: constraints on the timing of  
 686 Neoproterozoic and Palaeozoic tectonothermal events in the NW Highlands of Scotland:  
 687 *Journal of the Geological Society of London*, v. 158, p. 7-14.
- 688 Scherer E, Cameron K, Blichert-Toft J (2000) Lu–Hf garnet geochro- nology: closure  
 689 temperature relative to the Sm–Nd system and effects of trace mineral inclusions.  
 690 *Geochim Cosmochim Acta* 64(19):3413–3432
- 691 Scherer, E., Munker, C. & Mezger, K., 2001. Calibration of the lutetium-hafnium clock.  
 692 *Science (New York, N.Y.)*, 293(5530), pp.683–7. Available at:  
 693 <http://www.ncbi.nlm.nih.gov/pubmed/11474108> [Accessed August 14, 2014].
- 694 Skora, S., Baumgartner, L.P., Mahlen, N.J., Lapen, T.J., Johnson, C.M. & Bussy, F.,  
 695 2008. Estimation of a maximum Lu diffusion rate in a natural eclogite garnet. *Swiss*  
 696 *Journal of Geosciences*, 101, pp.637–650.
- 697 Smit M, Scherer E, Mezger K (2013) Lu–Hf and Sm–Nd garnet geo- chronology:  
 698 chronometric closure and implications for dating petrological processes. *Earth Planet*  
 699 *Sci Lett* 381:222–233



- 700 Stewart, A.D. 2002. The later Proterozoic Torridonian rocks of Scotland: their  
701 sedimentology, geochemistry and origin. Geological Society, London, Memoirs,  
702 **24**.
- 703 Storey, C.D., Brewer, T.S., and Parrish, R.R., 2004, Late Proterozoic tectonics in  
704 northwest Scotland: one contractional orogeny or several: *Precambrian Research*, v.  
705 134, p. 227-247.
- 706 Strachan, R.A., Smith, M., Harris, A.L. & Fettes, D.J. 2002. The Northern Highland and  
707 Grampian terranes. *In*: Trewin, N. (ed) *Geology of Scotland* (4<sup>th</sup> edition). Geological  
708 Society, London, 81-147.
- 709 Strachan, R.A., Nutman, A.P. & Friderichsen, J.D., 1995. SHRIMP U-Pb. *Journal of the*  
710 *Geological Society*, 13(152), pp.779–784.
- 711 Strachan, R.A., Holdsworth, R.E., Krabbendam, M. & Alsop, G.I. 2010. The Moine  
712 Supergroup of NW Scotland: insights into the analysis of polyorogenic supracrustal  
713 sequences. *In*: Law, R.D., Butler, R.W.H., Holdsworth, R.E., Krabbendam, M. &  
714 Strachan, R.A. (eds) *Continental Tectonics and Mountain Building: The Legacy of*  
715 *Peach and Horne*. Geological Society, Special Publications, **335**, 231-252.
- 716 Tanner, P.W.G. & Evans, J. A., 2003. Late Precambrian U-Pb titanite age for peak  
717 regional metamorphism and deformation (Knoydartian orogeny) in the western Moine,  
718 Scotland. *Journal of the Geological Society*, 160(4), pp.555–564. Available at:  
719 <http://jgs.lyellcollection.org/cgi/doi/10.1144/0016-764902-080> [Accessed August 14,  
720 2014].
- 721 Thirlwall, M.F. & Anczkiewicz, R., 2004. Multidynamic isotope ratio analysis using MC–  
722 ICP–MS and the causes of secular drift in Hf, Nd and Pb isotope ratios. *International*  
723 *Journal of Mass Spectrometry*, 235(1), pp.59–81. Available at:  
724 <http://linkinghub.elsevier.com/retrieve/pii/S1387380604001447> [Accessed August 14,  
725 2014].
- 726 Tinkham, D. K., Zuluaga, C. A. & Stowell, H. H. (2001) Metapelitic phase equilibria  
727 modelling in MnNCKFMASH: the effect of variable Al<sub>2</sub>O<sub>3</sub> and MgO/(MgO + FeO) on  
728 mineral stability. *Geological Materials Research*, 3, 1–42.
- 729 Trettin, H.P., Loveridge, W.D. & Sullivan, R.W. 1982. U-Pb ages on zircons from the  
730 M'Clintock West massif and the Markham Fjord plutonj, northernmost Ellesmere Island.  
731 *Current Research, Part C, Geological Survey of Canada Paper 82-1C*, p. 161-166.
- 732 Turnbull, M.J.M., Whitehouse, M.J., and Moorbath, S., 1996, New isotopic age  
733 determinations for the Torridonian, NW Scotland: *Journal of the Geological Society*,  
734 London, v. 153, p. 955-964.

- 735 van Breemen, O., Pidgeon, R.T. and Johnson, M.R.W., 1974, Precambrian and  
736 Palaeozoic pegmatites in the Moines of northern Scotland, *Journal of the Geological*  
737 *Society*, London, v. 130, p. 493-507.
- 738 Vance, D., Strachan, R.A. & Jones, K.A., 1998. Extensional versus compressional  
739 settings for metamorphism: Garnet chronometry and pressure-temperature-time  
740 histories in the Moine Supergroup, northwest Scotland. *Geology*, 26(10), pp.927–930.
- 741 Watt, G.R., Kinny, P.D., and Friderichsen, J.D., 2000, U-Pb geochronological of  
742 Neoproterozoic and Caledonian tectonothermal events in the East Greenland  
743 Caledonides: *Journal of the Geological Society*, London, v. 157, p. 1031-1048
- 744 Watt, G.R. & Thrane, K., 2001. Early Neoproterozoic events in East Greenland.  
745 *Precambrian Research*, 110(1-4), pp.165–184.
- 746 Wheeler, J., Park, R.G., Rollinson, H.R. & Beach, A. 2010. The Lewisian Complex:  
747 insights into deep crustal evolution. *In*: Law, R.D., Butler, R.W.H., Holdsworth, R.E.,  
748 Krabbendam, M. & Strachan, R.A. (eds). *Continental Tectonics and Mountain Building:*  
749 *The Legacy of Peach and Horne*. Geological Society, London, Special Publications,  
750 **335**, 51-79.
- 751 White, R.W., Powell, R. & Holland T.J.B., 2007. Progress relating to calculation of  
752 partial melting equilibria for metapelites. *Journal of Metamorphic Geology*, 25, 511–527.
- 753 White, RW, Powell, R, Holland, TJB, & Worley, B, 2000. The effect of TiO<sub>2</sub> and Fe<sub>2</sub>O<sub>3</sub>  
754 on metapelitic assemblages at greenschist and amphibolite facies conditions: mineral  
755 equilibria calculations in the system K<sub>2</sub>O–FeO–MgO–Al<sub>2</sub>O<sub>3</sub>–SiO<sub>2</sub>–H<sub>2</sub>O–TiO<sub>2</sub>–Fe<sub>2</sub>O<sub>3</sub>.  
756 *Journal of Metamorphic Geology*, 18, 497–511.